MAJOR PAPER

Characteristics of MR Imaging for Staging and Survival Analysis of Neuroendocrine Carcinoma of the Endometrium: A Multicenter Study in Japan

Kazuhiro Kitajima[1*], Takako Kihara[2], Yusuke Kawanaka[1], Junko Takahama[3],
Yoshiko Ueno[4], Takamichi Murakami[4], Kotaro Yoshida[5], Fumi Kato[6],
Akiko Takahata[7], Yoshihiko Fukukura[8], Jiro Munechika[9], Yasunari Fujinaga[10],
Takeru Fukunaga[11], Masahiro Tanabe[12], Yuichiro Kanie[13], Ayumu Kido[14],
Tsutomu Tamada[14], Rika Yoshida[15], Yuki Kamishima[16], and Koichiro Yamakado[1]

Purpose: This study aimed to examine MRI features and staging of neuroendocrine carcinoma (NEC) of the endometrium and evaluate survival.

Methods: Clinical data, pathological, and preoperative pelvic MRI findings in 22 patients with histologically surgery-proven endometrial NEC were retrospectively reviewed. Tumors were pure NEC ($n = 10$) or mixed histotype ($n = 12$), with 13 large and nine small cell type.

Results: International Federation of Gynecology and Obstetrics (FIGO) staging was I, II, III, and IV in 6, 2, 12, and 2 patients, respectively. In 13 (76.4%) of 17 patients with pathological deep myometrial invasion, MRI showed abnormal diffusely infiltrative high T_2 signal intensity throughout the myometrium with loss of normal uterine architecture. All tumors had restricted diffusion (apparent diffusion coefficient map low signal intensity, diffusion weighted imaging high signal intensity). Accuracy of T staging by MRI for all cases was 81.8%, with reference to pathology staging, while patient-based sensitivity, specificity, and accuracy for detecting metastatic pelvic lymph nodes was 60.0%, 100%, and 77.8%, respectively. Two intrapelvic peritoneal dissemination cases were detected by MRI. During follow-up (mean 30.4, range 3.3–138.4 months), 16 patients (72.7%) experienced recurrence and 12 (54.5%) died of disease. Two-year disease-free and overall survival rates for FIGO I, II, III, and IV were 66.7% and 83.3%, 50% and 100%, 10% and 33.3%, and 0% and 0%, respectively.

Conclusion: Abnormal diffusely infiltrative high T_2 signal intensity throughout the myometrium with normal uterine architecture loss and obvious restricted diffusion throughout the tumor are suggestive features of endometrial NEC. Pelvic MRI is reliable for intrapelvic staging of affected patients.

Keywords: *endometrial cancer, magnetic resonance imaging, neuroendocrine carcinoma, survival*

[1]Department of Radiology, Hyogo College of Medicine, Nishinomiya, Hyogo, Japan
[2]Department of Surgical Pathology, Hyogo College of Medicine, Nishinomiya, Hyogo, Japan
[3]Department of Radiology, Nara Medical University, Kashihara, Nara, Japan
[4]Department of Radiology, Kobe University Graduate School of Medicine, Kobe, Hyogo, Japan
[5]Department of Radiology, Graduate School of Medicine Science, Kanazawa University, Kanazawa, Ishikawa, Japan
[6]Department of Diagnostic and Interventional Radiology, Hokkaido University Hospital, Sapporo, Hokkaido, Japan

*Corresponding author: Department of Radiology, Hyogo College of Medicine, 1-1, Mukogawa-cho, Nishinomiya, Hyogo 663-8501, Japan. Phone: +81-798-45-6362, Fax: +81-798-45-6361, E-mail: kazu10041976@yahoo.co.jp

[7]Department of Radiology, Kyoto Prefectural University of Medicine, Kyoto, Kyoto, Japan
[8]Department of Radiology, Graduate School of Medical and Dental Sciences, Kagoshima University, Kagoshima, Kagoshima, Japan
[9]Department of Radiology, Showa University School of Medicine, Tokyo, Japan
[10]Department of Radiology, Shinshu University School of Medicine, Matsumoto, Nagano, Japan
[11]Department of Pathophysiological and Therapeutic Sciences, Tottori University, Yonago, Tottori, Japan
[12]Department of Radiology, Yamaguchi University Graduate School of Medicine, Ube, Yamaguchi, Japan
[13]Department of Radiology, Japanese Red Cross Society Himeji Hospital, Himeji, Hyogo, Japan
[14]Department of Radiology, Kawasaki Medical School, Kurashiki, Okayama, Japan
[15]Department of Radiology, Faculty of Medicine, Shimane University, Matsue, Shimane, Japan
[16]Department of Radiology, Nagoya City West Medical Center, Nagoya, Aichi, Japan

Introduction

A neuroendocrine carcinoma (NEC) of the female genital tract is an aggressive uncommon tumor usually involving the uterine cervix and ovaries, while endometrium occurrence is very rare.[1] An NEC of the uterine endometrium, an uncommon histologic subtype of endometrial carcinoma, is extremely rare and found in <1% of all primary endometrial carcinoma cases. The current World Health Organization (WHO) defines small cell NEC (SCNEC) as an undifferentiated carcinoma with cellular and nuclear features that include small-sized cells, scant cytoplasm, and hyperchromatic features, including inconspicuous finely granular and molded nuclei.[2] In contrast, a large cell NEC (LCNEC) is characterized by undifferentiated large cells lacking cytologic and architectural features of a small cell carcinoma, with glandular or squamous differentiation, and defined as a malignant tumor composed of large cells showing neuroendocrine differentiation.

An endometrial NEC is a highly malignant tumor and affected patients have an extremely poor prognosis.[3–6] Methods used for definitive diagnosis of a biopsy specimen from the endometrium are insensitive and inconclusive, because of tumor heterogeneity and non-specific pathological findings.[7] For diagnosis and staging of endometrial tumors, MRI is currently well established. If MRI can be shown to correctly diagnose endometrial NEC and provide accurate staging prior to treatment, it would be utilized as a helpful clinical tool. To the best of our knowledge, only four case reports discussing the MRI characteristics of endometrial LCNEC have been presented,[8–11] while none are known to include discussion of MRI findings of endometrial SCNEC, thus the MRI features of endometrial NEC are not well understood. The aim of this study was to identify distinct features as well as staging accuracy of endometrial NEC shown by MRI, including SCNEC and LCNEC. Furthermore, we evaluated survival of patients affected by this disease.

Materials and Methods

Patients

Ten institutions participated in this retrospective multicenter study of MRI findings of endometrial NEC in which 50% or more of component were NEC. The appropriate review board at each approved the study protocol and waived any informed patient consent requirement. Twenty-two patients (average age at diagnosis 63.4 years, range 39–82 years) with endometrial NEC underwent pre-operative pelvic MRI examinations between August 2004 and February 2018 at one of the participating institutions. For whole-body staging, 20 patients also underwent chest/abdomen/pelvis CT and two 18F-fluorodeoxyglucose-positron emission tomography/CT examinations. Additionally, four patients underwent an abdominal hysterectomy and bilateral salpingo-oophorectomy with or without an omentectomy, three an abdominal hysterectomy, bilateral salpingo-oophorectomy, and pelvic lymphadenectomy with or without an omentectomy, and 15 an abdominal hysterectomy, bilateral salpingo-oophorectomy, pelvic lymphadenectomy, and para-aortic lymphadenectomy with or without an omentectomy. Resected tumors and biopsy samples were processed for conventional hematoxylin–eosin and immunochemistry staining for various markers, including synaptophysin, chromogranin A, CD56, neuron-specific enolase (NSE), p53, SSRT2a, and Ki-67. Tumor staging was determined according to the 2008 International Federation of Gynecology and Obstetrics (FIGO) staging system for carcinomas of the endometrium.[12]

Pelvic MRI

Pelvic MRI was performed using a 1.5T system ($n = 17$) (1.5T Gyroscan Intera NT or Intera Achieva 1.5T nova dual; Philips Medical Systems, Best, the Netherlands; SIGNA HDxt 1.5T or SIGNA EXCITE; GE Healthcare, Waukesha, WI, USA. MAGNETON Vision, MAGNETON symphony, or MAGNETOM Avanto; Siemens Healthcare, Erlangen, Germany. NT MRT-200 SP5; Canon Medical Systems, Tochigi, Japan) or a 3.0T system ($n = 5$) (Intera Achieva Quasar dual; Philips Medical Systems. DISCOVERY MR750w or SIGNA EXCITE 3T-HD, GE Healthcare. MAGNETON Trio; Siemens Healthcare) using a body coil for excitation and pelvic phased-array coil for signal reception. At all institutions, butyl scopolamine (Buscopan; Boehringer Ingelheim, Tokyo, Japan) was given intramuscularly immediately before the examination to reduce artifacts from bowel peristalsis (unless contraindicated). The MRI parameters varied among the institutions. Unenhanced axial and sagittal fast-spin-echo T_2-weighted images (T_2WIs) were acquired with a TR/TE of 3400–4800/90–120 ms and a 4–5-mm slice thickness. Unenhanced spin-echo T_1-weighted images (T_1WIs) using a TR/TE of 532–699/7–11 ms and a 4–5-mm slice thickness were acquired in the axial and sagittal planes ($n = 12$) and axial or sagittal plane ($n = 10$). Axial diffusion weighted imaging (DWI) was performed in three orthogonal directions using spin-echo-type single-shot echo planar imaging with a 4–5-mm slice thickness and b-values of 0 and 1000 s/mm^2 ($n = 15$), 0 and 800 s/mm^2 ($n = 3$), 50 and 800 s/mm^2 ($n = 2$), 0 and 1500 s/mm^2 ($n = 1$) or 0, 500, and 1000 s/mm^2 ($n = 1$). Apparent diffusion coefficient (ADC) maps were made using all b-values. Twenty patients underwent contrast-enhanced scanning. In 15, after administration of 0.1 mmol/kg gadolinium diethylenetriaminepentaacetic acid (Gd-DTPA) at a rate of 2.0–3.0 mL/s, followed by a saline flush (15 mL at 2.0–3.0 mL/s), multiphase dynamic images with four phases ($n = 7$), three phases ($n = 4$), or five phases ($n = 4$) were scanned with fast-gradient-echo, fat-suppressed T_1-weighted, axial or sagittal sequences (2–3 mm slice thickness). Finally,

delayed (4–6 min after Gd-DTPA administration) T_1-weighted fat-suppressed axial and sagittal sequences were obtained sequentially, with parameters similar to those used before injection of Gd-DTPA. In the other 5 patients, after a single injection of Gd-DTPA at a dose of 0.1 mmol/kg body weight, T_1-weighted fat-suppressed axial and sagittal sequences in the late phase were obtained sequentially using parameters similar to those used prior to injection of Gd-DTPA.

Imaging analysis

All pelvic MRI were reviewed by 2 experienced radiologists (K.K. and Y.K. with 18 and 10 years of experience with gynecological MRI) who were blinded to patient information. MR images were presented on a Digital Imaging and Communications in Medicine viewer (Osirix; Pixmeo, Geneva, Switzerland). Tumor location, size, margin (well- or ill-defined), shape (mass-forming or endometrial thickness type), signal intensity (compared with uterine myometrium), lesion texture (homogeneous or heterogeneous), contrast enhancement patterns, and degrees were assessed. The greatest diameter in either the transverse or sagittal plane was used for tumor size determination. Dynamic contrast enhancement patterns were categorized as washout/plateau or gradual. Time-intensity curves were categorized into progressive, plateau, washout, and indeterminate types. Progressive enhancement was defined as a gradual increase in signal throughout all phases of enhancement. Plateau enhancement was defined as an initial increase in signal followed by a plateau in which the MRI signal units remained unchanged within a range of a 5% difference. A washout curve was defined as a steep initial increase and peak in signal followed by a decrease of at least 5–10%.[13] The degree of tumor enhancement in the late phase was compared with enhancement of normal myometrium and classified as mild, moderate, or strong. Decisions were reached by consensus.

The same 2 experienced readers also evaluated tumor extension into the myometrium, uterine serosa, cervical stroma, adnexa, parametrium, vagina, and urinary bladder or rectum mucosa, and pelvic lymph nodes (LNs), as well as distant metastasis to the bone and peritoneum using methods previously reported.[14,15] Lymphadenopathy was considered to be present based on size criteria (greater than 1 cm in short diameter) and/or signal intensity (with central necrosis).

Statistical analysis

Values are shown as the mean ± standard deviation (SD) and number (%). Analysis of disease-free survival (DFS) was done using Kaplan–Meier plots and a log-rank test, and defined as time from surgery to tumor recurrence or progression, as determined by histologic or follow-up findings including imaging. Overall survival (OS) was defined as the time interval from surgery to the date of death from this disease. Statistical analysis was performed using the SAS software package, version 9.3 (SAS Institute, Cary, NC, USA), with P-values <0.05 considered to indicate significance.

Results

Patient characteristics

The clinicopathologic features of the 22 patients in this study are summarized in Table 1. Patient age ranged from 39 to 82 years (median 67.0, mean 63.4 years). Presenting symptoms included vaginal bleeding ($n = 16$ patients), abnormal discharge ($n = 3$), uterine swelling ($n = 2$), and menstruation irregularity ($n = 1$). Abnormal levels of tumor markers included NSE in 4 (44.4%) of 9, proGRP in 1 (33.3%) of 3, CA125 in 6 (37.5%) of 16, CEA in 4 (22.2%) of 18, CA19-9 in 2 (11.8%) of 17, SCC in 1 (9.1%) of 11, AFP in 0 (0%) of 5,

Table 1 Patient and tumor characteristics

Character	n	Percentage (%)
Age at diagnosis (years)		
Median (range)	67.0 (39–82)	
NEC		
pure type	10	45.5
LCNEC	6	27.3
SCNEC	4	18.2
mixed with other histotype	12	54.5
LCNEC with other histotype	7	31.8
SCNEC with other histotype	5	22.7
Positivity for synaptophysin	19/20	95.0
Positivity for chromogranin A	15/19	78.9
Positivity for CD56	17/19	89.5
FIGO stage		
IA	2	9.1
IB	4	18.2
II	2	9.1
IIIA	1	4.5
IIIB	2	9.1
IIIC1	4	18.2
IIIC2	5	22.7
IVB	2	9.1
Treatment		
Surgery	2	9.1
Surgery + chemotherapy	15	78.9
Surgery + radiotherapy	2	9.1
Surgery + chemotherapy + radiotherapy	3	13.6

FIGO, Federation of Gynecology and Obstetrics; LCNEC, large cell neuroendocrine carcinoma; NEC, neuroendocrine carcinoma; SCNEC, small cell neuroendocrine carcinoma.

and CYFRA in 0 (0%) of 2 patients. Endometrial biopsy results revealed NEC in 10 (45.5%) of the present patients, whereas the preoperative pathological diagnoses were endometrioid adenocarcinoma in 8 patients (G1 in 4, G2 in 2, G3 in 2), undifferentiated carcinoma in 2 patients, and carcinosarcoma in 2 patients.

Pathological findings by the surgery showed pure NEC in 10 patients (45.5%), including pure LCNEC in 6 and SCNEC in 4. The remaining 12 (54.5%) had LCNEC combined with other pathologies, such as endometrioid adenocarcinoma or serous carcinoma (n = 7), or SCNEC combined with other pathologies, such as endometrioid adenocarcinoma or squamous cell carcinoma (n = 5).

All tumors were positive for one or more neuroendocrine markers (synaptophysin, chromogranin A, CD56). Immunohistochemical examinations of the specimens from patients examined for neuroendocrine markers yielded positive reactions for synaptophysin in 19 (95.0%) of 20, chromogranin A in 15 (78.9%) of 19, CD56 in 17 (89.5%) of 19, NSE in two (66.6%) of 3, p53 in 3 (60%) of 5, and SSRT2a in 1 (100%) of 1 patient. In addition, Ki-67 labelling index was identified in 5 patients and ranged from 7% to 90%, with a median of 46%. The mitotic index was high for 7 patients, ranging from 15 to 63 mitoses per 10 high power field (median 25.0). Lymphovascular invasion was observed in all of the present patients.

Eight patients were presented with early FIGO stage disease (stage IA, 2; stage IB, 4; stage II, 2) and 14 with advanced FIGO stage disease (stage IIIA, 1; stage IIIB, 2; stage IIIC1, 4; stage IIIC2, 5; stage IVB, 2). Two patients had peritoneal dissemination.

MRI findings

Magnetic resonance imaging findings are summarized in Table 2. The greatest tumor diameter was 62.0 ± 27.1 mm [mean ± SD] (range 25–123 mm). Sixteen (72.7%) tumors showed well-defined margins, while the remaining 6 (27.3%) had ill-defined margins. A mass-forming pattern was noted in 17 patients (77.3%) and the other 5 (22.7%) had an endometrial thickness pattern. In T_1WI results, 6 (27.3%) tumors showed slightly low signal intensity, 13 (59.1%) iso signal intensity, and 3 (13.6%) slightly high signal intensity. T_2WI results showed 15 (68.2%) tumors with slightly high signal intensity and 7 (31.8%) with high signal intensity. Images of 13 (76.4%) of 17 patients with pathologically deep myometrial invasion showed abnormal diffusely infiltrative high T_2 signal intensity throughout the myometrium along with loss of uterine normal architecture. All 22 tumors showed intense low signal intensity on ADC maps as well as intense high signal intensity on DWI throughout the mass. The internal tumor appearance was homogeneous in 12 (54.5%) cases and heterogeneous in 10 (45.5%). Dynamic contrast enhancement scanning results of 15 patients showed a gradual pattern in 12 (80.0%) and a washout/plateau pattern in 3 (20.0%). The degree of tumor

Table 2 MRI findings of endometrial neuroendocrine carcinoma

Character	n	Percentage (%)
Margin		
Well-defined	16	72.7
Ill-defined	6	27.3
Shape		
Mass-forming type	17	77.3
Endometrial thickness type	5	22.7
Internal appearance		
Homogeneous	12	54.5
Heterogeneous	10	45.5
T_1WI		
Slightly low	6	27.3
Iso	13	59.1
Slightly high	3	13.6
T_2WI		
Slightly high	15	68.2
High	7	31.8
Diffusion weighted imaging		
Intense high	22	100
Apparent diffusion coefficient map		
Intense low	22	100
Dynamic contrast enhancement pattern		
Gradual pattern	12	80.0
Washout/plateau pattern	3	20.0
The enhancement degree on the late phase		
Mild	16	80.0
Moderate	4	20.0

T_1WI, T_1-weighted image; T_2WI, T_2-weighted image.

enhancement in the late phase was mild for 16 tumors (80.0%) and moderate for four (20.0%). Two representative cases are presented in Figs. 1 and 2.

MRI and pathological staging

Findings of MRI diagnostic accuracy of tumor extension in neighboring organs are summarized in Table 3. All 22 patients showed myometrial invasion proven pathologically and MRI was able to detect that in 18 (81.8%). Furthermore, deep myometrial (≥1/2) invasion was noted in 17 (77.3%) and correctly detected by MRI in 14 (Fig. 1). On the other hand, 2 of 5 patients without deep myometrial invasion were incorrectly over-diagnosed by MRI (Fig. 2). Cervical stroma invasion was pathologically clarified in 10 (45.5%) of 22 patients and correctly detected in 7 patients by MRI, while uterine serosa invasion was pathologically clarified in 7 (31.8%) and correctly detected in 5, adnexa invasion was pathologically clarified in 6 (27.3%) and correctly detected
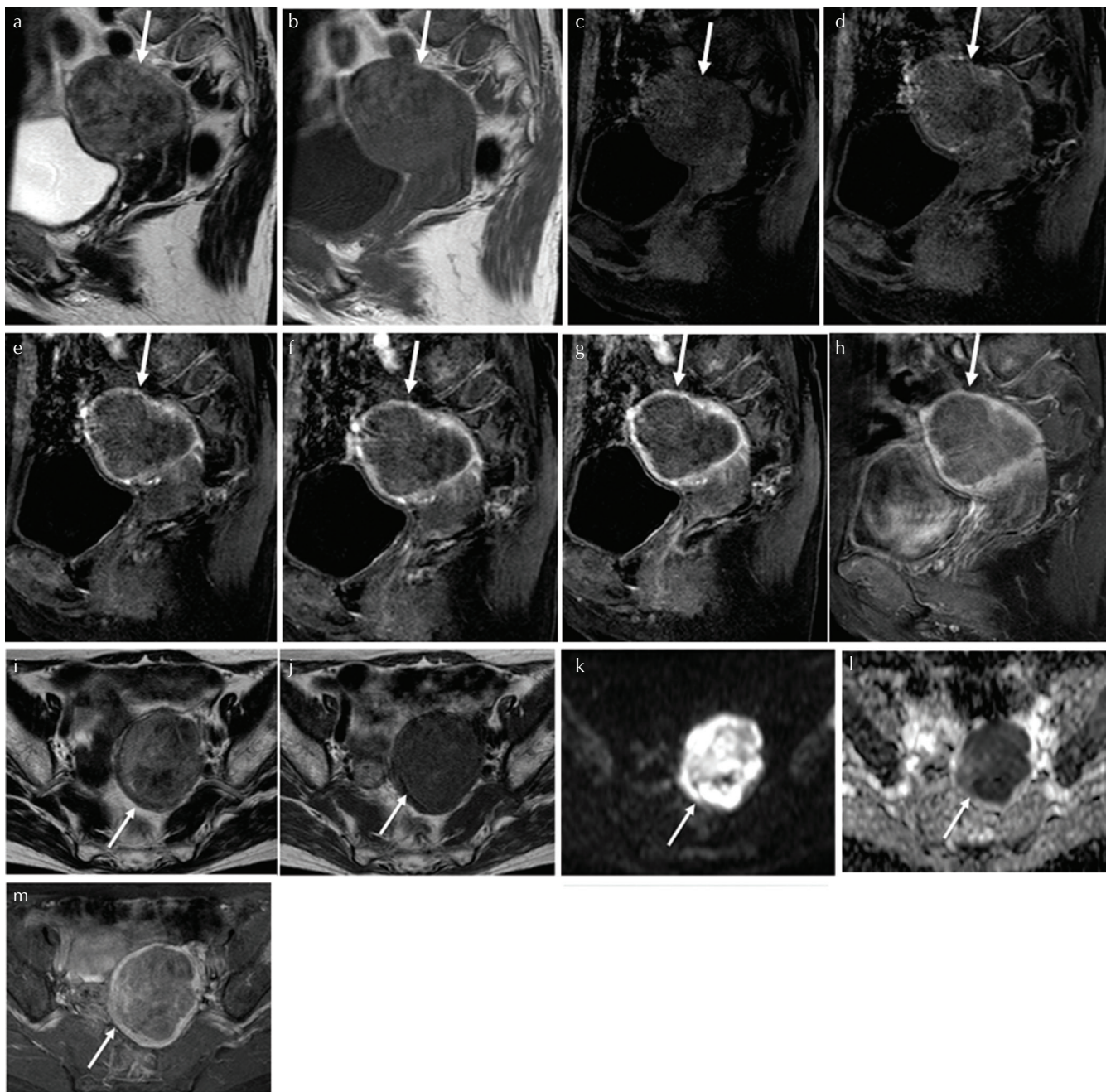
Fig. 1 A 69-year-old woman with pT1bN0M0 and FIGO stage IB endometrial small cell neuroendocrine carcinoma. (**a**) Sagittal T_2WI showing abnormal diffuse infiltrative heterogeneous and slightly high signal intensity throughout the myometrium, along with loss of normal uterine architecture (arrow). (**b**) Sagittal T_1WI showing mild enlargement of uterine body (arrow). Dynamic contrast-enhanced axial fat-suppressed T_1WI, including (**c**) pre-contrast, and (**d**) 30, (**e**) 60, (**f**) 120, and (**g**) 180 s following administration of Gd-DTPA, demonstrating a weak and gradual enhancement pattern in the tumor (arrow*s*). (**h**) Sagittal late-phase enhanced fat-suppressed T_1WI (240 s after Gd-DTPA administration) showing weak enhancement of tumor invading deep into myometrium (arrow). (**i**) Axial T_2WI showing abnormal diffuse infiltrative heterogeneous and slightly high T_2 signal intensity throughout the myometrium, along with loss of normal uterine architecture (arrow). (**j**) Axial T_1WI showing mild enlargement of uterine body (arrow). (**k**) Axial DWI showing uterine mass involving both endometrium and myometrium, with remarkably high signal intensity throughout the tumor (arrow). (**l**) Axial Apparent diffusion coefficient (ADC) map showing obvious diffusion restriction of uterine body tumor (arrow). (**m**) Axial late-phase enhanced fat-suppressed T_1WI obtained 6 min after Gd-DTPA showing weak enhancement of uterine tumor invading deep into myometrium (arrow). Deep myometrial invasion of the primary tumor was confirmed by surgical pathology findings. The patient showed progression at 42.1 months and died 78.6 months after surgery. ADC, apparent diffusion coefficient; DWI, diffusion weighted imaging; FIGO, Federation of Gynecology and Obstetrics; Gd-DTPA, gadolinium diethylenetriaminepentaacetic acid; T_1WI, T_1-weighted image; T_2WI, T_2-weighted image.
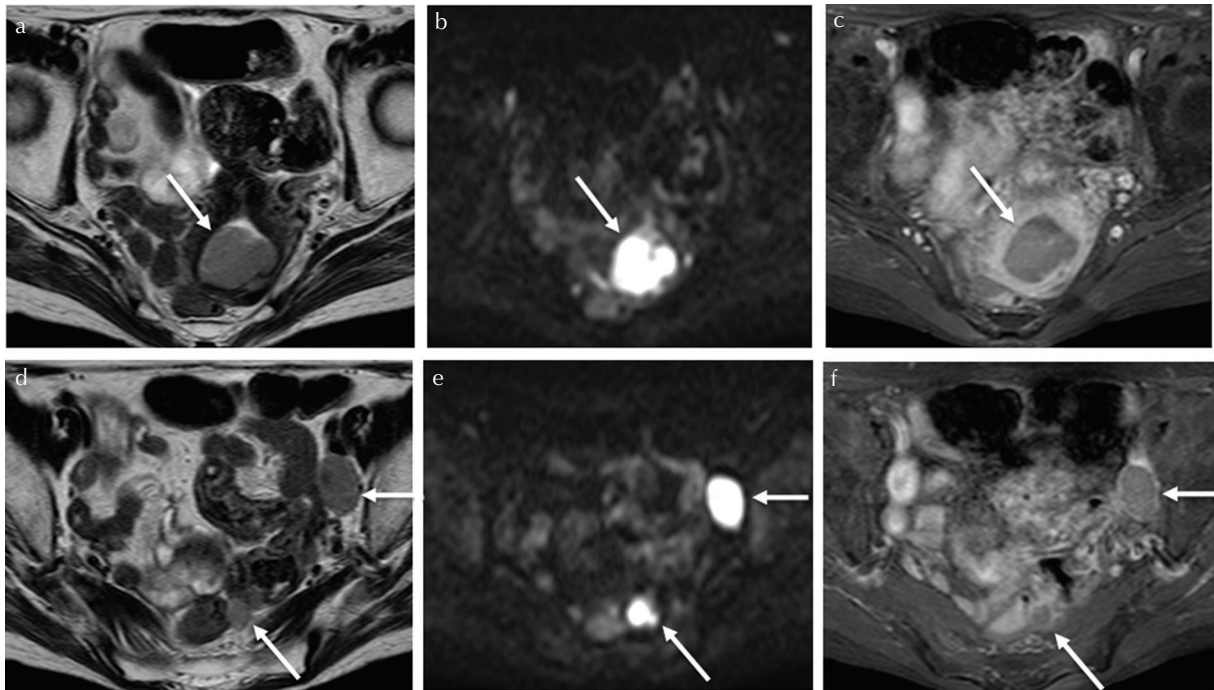
Fig. 2 A 65-year-old woman with pT3aN1M1 (peritoneal dissemination) and FIGO stage IV and endometrial small cell neuroendocrine carcinoma. (**a**) Axial T$_2$WI showing slightly hyperintense and homogeneous mass invading from endometrium to myometrium (arrow). Deep myometrial invasion (>50%) was suspected. (**b**) Axial DWI showing remarkably high signal intensity throughout tumor (arrow). (**c**) Axial late-phase enhanced fat-suppressed T$_1$WI obtained 5 min after Gd-DTPA administration showing weak enhancement of tumor (arrow). (**d**) Axial T$_2$WI showing swollen lymph node, exceeding 1 cm in the short diameter, in the left obturator area (upper arrow), suggesting nodal metastasis, along with a slightly hyperintense peritoneal mass 1 cm in size (lower arrow), indicating peritoneal dissemination. (**e**) Axial DWI showing remarkably high signal intensity in the left obturator node (upper arrow) and peritoneal mass (lower arrow), indicating node metastasis and peritoneal dissemination, respectively. (**f**) Axial late-phase enhanced fat-suppressed T$_1$WI obtained 5 min after Gd-DTPA administration showing weak enhancement of left obturator node (upper arrow) and peritoneal mass (lower arrow), confirming node metastasis and peritoneal dissemination, respectively. Myometrial invasion of the primary tumor (<50%), invasion of left adnexa left obturator node metastasis, and peritoneal dissemination were confirmed by surgical pathology findings. The patient showed recurrence at 7.5 months and died 12.1 months after surgery. DWI, diffusion weighted imaging; FIGO, Federation of Gynecology and Obstetrics; Gd-DTPA, gadolinium diethylenetriaminepentaacetic acid; T$_1$WI, T$_1$-weighted image; T$_2$WI, T$_2$-weighted image.

Table 3 MRI staging of endometrial neuroendocrine carcinoma on a per patient basis

	Sensitivity	Specificity	PPV	NPV	Accuracy
Myometrial invasion	81.8% (18/22)	-	100% (18/18)	-	81.8% (18/22)
95% CI	65.7–97.9	-	100	-	65.7–97.9
Deep myometrial invasion (≥50%)	82.3% (14/17)	60.0% (3/5)	87.5% (14/16)	50.0% (3/6)	77.3% (17/22)
95% CI	64.2–100	57.6–84.5	71.3–100	17.3–82.7	59.8–94.8
Invasion of cervical stroma	70.0% (7/10)	91.7% (11/12)	87.5% (7/8)	78.6% (11/14)	81.8% (18/22)
95% CI	41.6–98.4	76.0–100	64.6–100	57.1–100	65.7–97.9
Invasion of uterine serosa	71.4% (5/7)	100% (15/15)	100% (5/5)	88.2% (15/17)	90.9% (20/22)
95% CI	38.0–100	100	100	72.9–100	78.9–100
Invasion of adnexa	83.3% (5/6)	100% (16/16)	100% (5/5)	94.1% (16/17)	95.5% (21/22)
95% CI	53.5–100	100	100	82.9–100	86.7–100
Invasion of parametrium	50.0% (1/2)	100% (20/20)	100% (1/1)	95.2% (20/21)	95.5% (21/22)
95% CI	0–100	100	100	86.1–100	86.7–100
Metastatic pelvic lymph node	60.0% (6/10)	100% (8/8)	100% (6/6)	75.0% (8/12)	77.8% (14/18)
95% CI	29.6–90.4	100	100	45.0–100	65.7–97.9
Peritoneal dissemination	100% (2/2)	100% (20/20)	100% (2/2)	100% (20/20)	100% (22/22)
95% CI	100	100	100	100	100

PPV, positive predictive value; NPV, negative predictive value; CI, confidence interval.

in 5, and parametrium invasion was pathologically clarified in 2 and correctly detected in 1. No vaginal, urinary bladder, or rectum mucosa invasion was observed in any of our cases.

According to the most recent report of the American Joint Committee on Cancer (AJCC) cancer staging,[16] T stage was classified as pT1a in 3, pT1b in 6, pT2 in 3, pT3a in 8, and pT3b in 2 patients. Agreements between MRI staging and pathological staging are shown in Table 4. Two patients with pathological myometrial invasion of <50% have also proved to have pathological cervical stroma invasion (pT2) in 1 patient and pathological adnexal invasion (pT3a) in 1 patient. Agreement was noted in 18 patients, with an overall accuracy of MRI for local staging of 81.8%. A discrepancy occurred in 4 patients that resulted from false negative findings for pT1b (*n* = 1), pT2 (*n* = 1), pT3a (*n* = 1), and pT3b (*n* = 1).

Pelvic lymph nodal metastasis was pathologically clarified in 10 (55.5%) of the 18 patients who had undergone lymphadenectomy and correctly detected in 6 patients by MRI. The values for patient-based sensitivity, specificity, positive predictive value (PPV), negative predictive value (NPV), and accuracy for detecting metastatic pelvic LN were 60.0% (6/10), 100% (8/8), 100% (6/6) 75.0% (8/12), and 77.8% (14/18), respectively (Table 3 and Fig. 2).

Survival analysis

After surgery, 15 patients received adjuvant chemotherapy, 3 chemoradiation therapy, 2 radiation therapy, and 2 no therapy. During a mean follow-up period of 30.4 months (3.3–138.4 months), 16 (72.7%) experienced recurrence. Of those, 2 (33.3%) of 6 patients classified as FIGO I, 1 (50.0%) of 2 as FIGO II, 11 (91.7%) of 12 as FIGO III, and 2 (100%) of 2 as FIGO IV had recurrence. The sites of recurrence in these 16 patients were LN (*n* = 4), peritoneum (*n* = 4), local (*n* = 2), brain (*n* = 1), liver and lung (*n* = 1), liver and peritoneum (*n* = 1), LN, lung, and liver (*n* = 1), LN, lung, and bone (*n* = 1), and LN, lung, adrenal gland, and brain (*n* = 1).

The median time to recurrence in the 16 patients was 6.75 months (range 1.5–20.2 months). Two-year DFS rates for patients classified as FIGO I, II, III, and IV were

66.7% (4/6), 50.0% (1/2), 8.3% (1/12), and 0% (0/2), respectively, while that was 27.3% (6/22) for all patients. The 14 patients with advanced FIGO stage disease (III and IV) showed significantly shorter PFS as compared with the 8 with early FIGO staged disease (I and II, *P* = 0.0005; Fig. 3).

During a mean follow-up period of 30.4 months (3.3–138.4 months), 12 (54.5%) of the 22 patients died of disease, including 1 (16.7%) classified as FIGO I, zero (0%) as FIGO II, 9 (75.0%) as FIGO III, and 2 (100%) as FIGO IV. Median OS for all patients was 22.6 months, while that was 26.1 months for FIGO I, 80.9 months for FIGO II, 18.9 months for FIGO III, and 9.8 months for FIGO IV classifications. Additionally, the 2-year OS rate for FIGO I, II, III, and IV was 83.3% (5/6), 100% (2/2), 33.3% (4/12), and 0% (0/2), respectively, while that was 50.0% (11/22) for all patients. The 14 patients with advanced FIGO stage disease (III and IV) showed significantly worse OS as compared with the 8 with early FIGO stage disease (I and II, *P* = 0.0028; Fig. 4).

Discussion

The present analysis of 22 patients with histologically and surgery proven endometrial NEC provides important information in regard to MRI findings and patient prognosis. An abnormal diffuse infiltrative high T_2 signal intensity throughout the myometrium with loss of uterine normal architecture and obvious restricted diffusion throughout the tumor are likely suggestive features of endometrial NEC. Furthermore, pelvic MRI is reliable for intrapelvic staging of endometrial NEC, which has a poor prognosis, especially advanced stage patients.
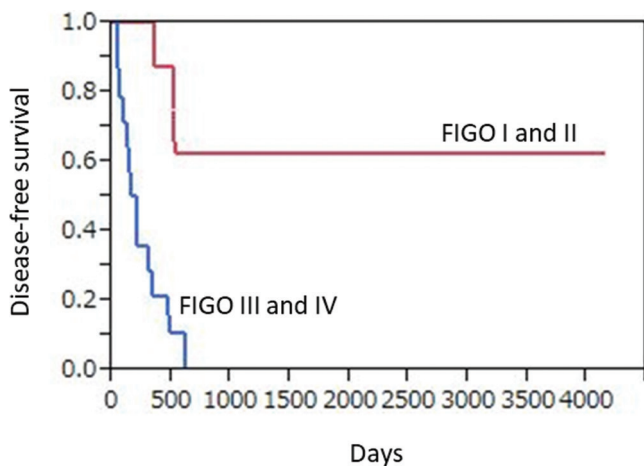
Table 4 Correlation between MRI T staging and pathological staging in patients with endometrial neuroendocrine carcinoma

MRI staging	Pathological staging						
	T1a	T1b	T2	T3a	T3b	T4	All
T1a	3	1	1	0	0	0	5
T1b	0	5	0	1	0	0	6
T2	0	0	2	0	1	0	3
T3a	0	0	0	7	0	0	7
T3b	0	0	0	0	1	0	1
T4	0	0	0	0	0	0	0
All	3	6	3	8	2	0	22

Fig. 3 Kaplan–Meier progression-free survival curves for 22 patients with endometrial neuroendocrine carcinoma according to FIGO stage. Patients with advanced FIGO stage disease (III and IV, *n* = 14) showed significantly shorter DFS as compared with those with early FIGO stage disease (I and II; *n* = 8, *P* = 0.0005). DWI, diffusion weighted imaging; FIGO, Federation of Gynecology and Obstetrics.
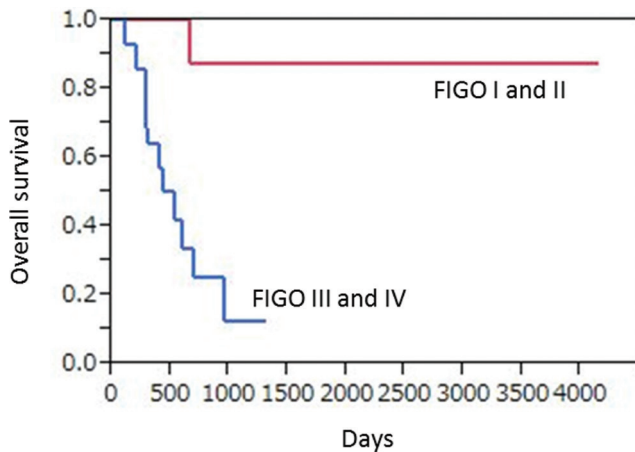
Fig. 4 Kaplan–Meier overall survival curves for 22 patients with endometrial neuroendocrine carcinoma according to FIGO stage. Patients with advanced FIGO stage disease (III and IV, *n* = 14) showed significantly worse OS as compared with those with early FIGO stage disease (I and II; *n* = 8, *P* = 0.0028). FIGO, Federation of Gynecology and Obstetrics; OS, overall survival.

We compared 4 previous case reports that discussed MRI findings of endometrial LCNEC[8–11] and found similar findings in the present patients, as follows: (1) The tumors showed diffuse involvement of both the endometrium and myometrium, and an ill-defined endometrial–myometrial border was seen with loss of normal architecture; (2) the masses showed diffusely infiltrative and heterogeneous high signal intensity on T_2WI; (3) DWI showed abnormal high signal intensity throughout the tumors, reflecting high cellularity of malignant cells. MRI findings of endometrial NEC mimic those of other types of cancer, including type II endometrial carcinoma (poorly differentiated endometrioid carcinoma, papillary serous carcinoma, clear cell carcinoma),[17] a malignant tumor of the uterine corpus that invades the endometrium, malignant lymphoma, endometrial carcinosarcoma, uterine sarcoma, and metastatic cancer. Definitive diagnosis based on preoperative MRI findings is difficult.

The average age of 42 patients with endometrial SCNEC at the time of diagnosis was reported to be 60 years old,[3] while Ogura et al.[11] noted ages ranging from 40 to 88 years (mean 62 years) for 19 cases of endometrial LCNEC. In a series of 25 patients with endometrial NEC (LCNEC 15, SCNEC 4, mixture of both 6), patient age ranged from 37 to 87 years (median 57 years).[7] A comparison showed that the average age of the present cases (63.4 years) was about 10 years older than that of endometrial adenocarcinoma cases.[4]

The clinical behavior of NEC of the endometrium is aggressive and highly malignant, with an advanced stage commonly observed at the time of diagnosis. To date, 83 known cases of endometrial SCNEC have been reported in English literature, of which 40.8% (29 of 71) were FIGO stage I or II and 59.2% (42 of 71) stage III or IV among cases with available staging data.[3] In a series of 25 patients with endometrial NEC, Pocrnich et al.[7] found that most (68%)

were advanced stage (FIGO III or IV). Similar to those reports, our investigation showed an advanced stage for about two-thirds (63.6%) of the present cases.[7]

Patients with NEC of the endometrium have been reported to have a poor prognosis. In a literature review, Katahira et al.[4] found that only 23% (3/13) of endometrial SCNEC patients with stage I disease died of the disease within 5 years, while 73% (17/22) of those with stage II–IV died within 2 years of diagnosis. In addition, Korcum et al.[5] reviewed 19 endometrial SCNEC cases with stage I disease, including one under their care and 18 others previously reported. Of those, 13 (68.4%) patients had no evidence of disease at the time of follow-up and there were four (21.1%) long-term survivors with no evidence of disease after 5 years. FIGO stage is the most important prognostic factor. Matsumoto et al.[6] published a review of long-term survivors (>1 year) diagnosed with endometrial SCNEC. Of 53 with detailed information available, 20 (37.7%) patients were long-term survivors, including 17 (85.0%) with stage I or II disease, and only 3 (15.0%) with stage III or IV disease. In that study, 4 (66.7%) of 6 patients survived more than 1 year after surgery and 2 of those 4 had advanced stage IIIB or IIIC disease. Similar to these reports, our study also demonstrated a 2-year OS rate of 87.5% for early-stage disease (I or II) as compared with 28.6% for advanced-stage (III or IV).

Neuroendocrine carcinoma of the uterine body is rarely encountered, though affected patients have a poor prognosis and no treatment strategy has been established. Although clear treatment recommendations for endometrial NEC have not been defined, patients should be given multimodality therapy, including surgery, chemotherapy and radiotherapy,[3–5] with surgery generally accepted to be the cornerstone. As for chemotherapy, patients are generally administered 6 cycles of cisplatin (60 mg/m^2, day 1) and etoposide (60 mg/m^2, days 1, 8, and 15).[7,8]

Our study had several limitations. First, our study include its retrospective design and variations in the MRI scanning protocols among the centers over the 14-year study period, primarily due to the rarity of this entity. Second, the pathological diagnosis of 22 endometrial NECs was made by each pathologist at each institution, not by one pathologist (central diagnosis).

Conclusion

Neuroendocrine carcinoma of the uterine endometrium is a rare disease and affected patients show poor prognosis, especially those in an advanced stage. Definitive diagnosis based on preoperative MRI results is difficult. However, abnormal diffuse infiltrative high T_2 signal intensity throughout the myometrium with loss of uterine normal architecture and obvious restricted diffusion throughout the tumor may suggest endometrial NEC. Pelvic MRI is a reliable imaging technique for intrapelvic staging of endometrial NEC.

Funding

Acknowledgments

Conflicts of Interest

All authors declare no actual or potential conflicts of interest.

References

1. Rouzbahman M, Clarke B. Neuroendocrine tumors of the gynecologic tract: select topics. Semin Diagn Pathol 2013; 30:224–233.
2. Kurman RJ, Carcanju ML, Herrington CS, Young, RH. World Health Organization classification of tumours of female reproductive organs. 4th ed. Lyon: IARC Press; 2014.
3. Koo YJ, Kim DY, Kim KR, et al. Small cell neuroendocrine carcinoma of the endometrium: a clinicopathologic study of six cases. Taiwan J Obstet Gynecol 2014; 53:355–359.
4. Katahira A, Akahira J, Niikura H, et al. Small cell carcinoma of the endometrium: report of three cases and literature review. Int J Gynecol Cancer 2014; 14:1018–1023.
5. Korcum AF, Aksu G, Ozdogan M, Erdogan G, Taskin O. Stage I small cell carcinoma of the endometrium: survival and management options. Acta Obstet Gynecol Scand 2008; 87:122–126.
6. Matsumoto H, Takai N, Nasu K, Narahara H. Small cell carcinoma of the endometrium: a report of two cases. J Obstet Gynaecol Res 2011; 37:1739–1743.
7. Pocrnich CE, Ramalingam P, Euscher ED, Malpica A. Neuroendocrine carcinoma of the endometrium: a clinicopathologic study of 25 cases. Am J Surg Pathol 2016; 40:577–586.
8. Makihara N, Maeda T, Nishimura M, et al. Large cell neuroendocrine carcinoma originating from the uterine endometrium: a report on magnetic resonance features of 2 cases with very rare and aggressive tumor. Rare Tumors 2012; 4:e37.
9. Nguyen ML, Han L, Minors AM, et al. Rare large cell neuroendocrine tumor of the endometrium: a case report and review of the literature. Int J Surg Case Rep 2013; 4:651–655.
10. Kobayashi A, Yahata T, Nanjo S, et al. Rapidly progressing large-cell neuroendocrine carcinoma arising from the uterine corpus: a case report and review of the literature. Mol Clin Oncol 2017; 6:881–885.
11. Ogura J, Adachi Y, Yasumoto K, et al. Large-cell neuroendocrine carcinoma arising in the endometrium: a case report. Mol Clin Oncol 2018; 8:571–574.
12. Pecorelli S. Revised FIGO staging for carcinoma of the vulva, cervix, and endometrium. Int J Gynaecol Obstet 2009; 105:103–104.
13. Garza A, Elsherif SB, Faria SC, et al. Staging MRI of uterine malignant mixed Müllerian tumors versus endometrial carcinomas with emphasis on dynamic enhancement characteristics. Abdom Radiol (NY) 2020; 45:1141–1154.
14. Freeman SJ, Aly AM, Kataoka MY, Addley HC, Reinhold C, Sala E. The revised FIGO staging system for uterine malignancies: implications for MR imaging. Radiographics 2012; 32:1805–1827.
15. Rauch GM, Kaur H, Choi H, et al. Optimization of MR imaging for pretreatment evaluation of patients with endometrial and cervical cancer. Radiographics 2014; 34:1082–1098.
16. Edge SB, Compton CC. The American joint committee on cancer: the 7th edition of the AJCC cancer staging manual and the future of TNM. Ann Surg Oncol 2010; 17: 1471–1474.
17. Fukunaga T, Fujii S, Inoue C, et al. Accuracy of semiquantitative dynamic contrast-enhanced MRI for differentiating type II from type I endometrial carcinoma. J Magn Reson Imaging 2015; 41:1662–1668.